Best Practices for Comparing Ocean Turbulence Measurements across Spatiotemporal Scales

CAITLIN B. WHALEN[a]

[a] *Applied Physics Laboratory, University of Washington, Seattle, Washington*

(Manuscript received 28 October 2020, in final form 23 December 2020)

ABSTRACT: The turbulent energy dissipation rate in the ocean can be measured by using rapidly sampling microstructure shear probes, or by applying a finescale parameterization to coarser-resolution density and/or shear profiles. The two techniques require measurements that are on different spatiotemporal scales and generate dissipation rate estimates that also differ in spatiotemporal scale. Since the distribution of the measured energy dissipation rate is closer to lognormal than normal and fluctuates with the strength of the turbulence, averaging the two approaches on equivalent spatiotemporal scales is critical for accurately comparing the two methods. Here, microstructure data from the 1997 Brazil Basin Tracer Release Experiment (BBTRE) is used to demonstrate that comparing averages of the dissipation rate on different spatiotemporal scales can generate spurious discrepancies of up to a factor of order 10 in regions of strong turbulence and smaller biases of up to a factor of 2 in the presence of weaker turbulence.

SIGNIFICANCE STATEMENT: Ocean turbulence is more commonly weak than strong. This implies that measurements of ocean turbulence that are made over small time and length scales will measure weak turbulence more often than those that measure turbulence averaged over a large area and a long time. Therefore, comparing the two measurement methods can lead to a mismatch that is due to the statistics of turbulence opposed to inherent differences in the methods. While it is important for oceanographers to compare different measurement methods, care needs to be taken to ensure that equivalent quantities are being compared. This note is important since it explains a key consideration necessary for accurately comparing ocean turbulence measurements.

KEYWORDS: Mixing; In situ oceanic observations; Sampling

1. Introduction

Finescale parameterizations are often used to estimate the energy dissipation rate and diapycnal diffusivity by leveraging profiles of commonly measured density and/or velocity (Gregg 1989; Wijesekera et al. 1993; Polzin et al. 1995; Kunze et al. 2006; Whalen et al. 2012; Kunze 2017). Measurements of internal wave shear or strain with resolutions of one to tens of meters are first used to calculate the energy level of the local internal wave field; then finestructure parameterization methods are applied to estimate the associated expected dissipation rate on vertical length scales of hundreds of meters and time scales of tens of hours (Henyey et al. 1986; Müller et al. 1986; Henyey and Pomphrey 1983; Gregg 1989; Winkel et al. 2002; Polzin et al. 2014). The finescale methods rely on two overarching assumptions (Whalen et al. 2015): first, that all of the observed strain and/or shear is due to open ocean internal waves (i.e., a "Garrett–Munk" internal wave field exists), and second, that the local turbulence is primarily caused by internal waves opposed to other dynamical sources of turbulence.

Another way to estimate the turbulent energy dissipation rate is to use microstructure measurements taken by quickly sampling shear probes that generate profiles of shear with centimeter-scale resolution (Oakey 1982; Gregg 1999). The spectra of these shear measurements are then compared with the theoretical isotropic turbulence spectra (Nasmyth 1973) to generate estimates of the dissipation rate on spatial scales of meters and time scales of minutes. The dissipation rate estimates can then be combined with density profiles to estimate the diapycnal diffusivity (Osborn 1980).

There are two key repercussions of the inherent difference between the spatiotemporal scales of the microstructure and finestructure estimation methods. First, fewer assumptions are needed to calculate the dissipation rate using microstructure methods than are necessary when using finescale methods, implying that the microstructure will provide estimates that are accurate over a larger range of conditions (as summarized in Polzin et al. 2014). Second, the two methods calculate dissipation rates over different spatiotemporal scales, so the estimates that are generated are not directly equivalent, which is the topic of this note. The temporal scales matter because the turbulence at one location can vary over many orders of magnitude as an internal wave passes by (Gregg et al. 1993) and a similarly dramatic variability is also observed in space (Moum et al. 1995). In this variable environment a single microstructure profile can be used to estimate essentially a *snapshot* of the dissipation rate, in contrast to the very different turbulent field observed by finestructure which (at best) can only produce an estimate of the average energy dissipation rate observed on the spatiotemporal scales of passing internal waves.

When microstructure measurements of the dissipation rate are averaged over similar spatiotemporal scales as open-ocean finestructure, the two methods agree (Gregg 1989; Polzin et al. 1995; Whalen et al. 2015). For example, in one study 81% of

Denotes content that is immediately available upon publication as open access.

Corresponding author: Caitlin B. Whalen, cbwhalen@uw.edu

DOI: 10.1175/JTECH-D-20-0175.1

comparisons between finestructure and microstructure agreed within a factor of 2 and 96% agreed within a factor of 3 (Whalen et al. 2015). In contrast, when microstructure measurements on smaller space, time, or spatiotemporal scales are compared to finestructure measurements a distinct pattern emerges: the two methods appear to agree well at lower dissipation rates; however, in the presence of energetic turbulence the finestructure method appears to overestimate the dissipation rate (e.g., Waterman et al. 2014; Ijichi and Hibiya 2015; Takahashi and Hibiya 2019). Here I draw on the statistics of dissipation rate measurements detailed in Gregg et al. (1993) and Davis (1996) to describe how this apparent discrepancy can be explained at least in part by the disparity in spatiotemporal averaging between the two different types of measurement approaches used in these studies.

2. An example

Microstructure data from the 1997 Brazil Basin Tracer Release Experiment (BBTRE) (Ledwell et al. 2000; Polzin et al. 1997; St. Laurent et al. 2001) is used to explore the ramifications of averaging the dissipation rate on different spatiotemporal scales. Quality controlled dissipation rate measurements from BBTRE are publicly available in 0.5 m bins through the NSF-funded Microstructure Database. BBTRE was chosen for this note because the dataset spans a large range of dissipation rates, including strong turbulence over the rough Mid-Atlantic Ridge and weaker turbulence over the Brazil Basin.

The BBTRE microstructure data from the database is averaged over different spatial and temporal scales as follows where each average requires at least 10 dissipation rate estimates:

1) Option A—Temporal averaging only, ϵ_{PT}: Groups of five consecutive dissipation rate profiles that have a vertical resolution of 10 m are averaged together (each profile is separated by a mean of 0.3 days), approximating the temporal averaging in finestructure estimates but not the vertical spatial averaging.
2) Option B—Spatial averaging only, ϵ_{PS}: Each individual profile is averaged into 200 m vertical bins, a typical length scale of finescale estimates, but no temporal averaging is incorporated.
3) Option C—Minimal averaging, ϵ_{10}: Each individual dissipation rate profile is averaged into 10 m bins (i.e., minimal averaging in space but none in time).
4) Option D—Spatiotemporal ''finescale'' averaging, ϵ_F: Microstructure profiles are averaged in time as in option A and in space as in option B to approximate the spatiotemporal scales of the dissipation rates estimated using the finescale parameterization.

These options comprise a framework used to highlight the range of choices made in previous studies; on one extreme a study may temporally average but does not average over vertical spatial scales large enough to be equivalent to finescale estimates (option A), while on another extreme a study may compare individual profiles with vertical-length-scale averaging equivalent to finescale approaches (option B). The studies mentioned here (Waterman et al. 2014; Ijichi and Hibiya 2015; Takahashi and Hibiya 2019) chose a combination: essentially option B but with vertical length scales that are smaller than their finescale estimates. The terminology of ''temporal averaging only'' and ''spatial averaging only'' indicates that these options are averaged in time or in space to be equivalent to ''finescale'' averages, and any other averaging is very small compared to spatiotemporal scales of finescale estimates.

The BBTRE microstructure data demonstrates that the ''finescale'' averaged dissipation rate is typically larger than both of the options that apply only partial averaging: time-only and space-only (Fig. 1). For the time-only averaging option, the majority (65%) of the ''finescale'' averaged dissipation rates are larger than the partially averaged dissipation rates; i.e., they fall above the 1-to-1 line in the joint probability density function (PDF) (Fig. 1a). Similarly for the space-only case, 60% of ''finescale'' averaged dissipation rates are larger than the space-only averages (Fig. 1b).

The largest discrepancy between the ''finescale'' averaged and the time-only or space-only dissipation rates occurs when the dissipation rate is high, and only a slight discrepancy is observed when the dissipation rate is low (Fig. 1c). For example, in Fig. 1c, a ''finescale'' averaged dissipation rate of 10^{-9} W kg^{-1} or greater is a factor of 2–17 larger than the time-only averaged value and a factor of 2–16 larger than the space-only averaged value. When the ''finescale'' averaged dissipation rate drops below 10^{-9} W kg^{-1}, it is only a factor of 1–2 larger than the partially averaged value. The same general pattern holds for the minimally averaged dissipation rate (not shown), which has a larger number of samples contributing to the mean factor difference. Therefore, the discrepancy is a function of the spatiotemporally averaged (i.e., ''finescale'' averaged) dissipation rate, with larger discrepancies in the presence of energetic turbulence.

3. Discussion

If the dissipation rate were a normally distributed variable, comparing values that are averaged on different spatiotemporal scales would produce a larger ''spread'' in the comparison plots, leading to a pattern that would be easy to interpret. However, since the microstructure data distribution is closer to lognormal, as shown in Gregg et al. (1993), the mean is larger than the median. This near-lognormality causes a systematic bias when a partially averaged variable is compared with the mean (Davis 1996), manifesting in Figs. 1a and 1b as a larger percentage of averages above the 1-to-1 line.

While the measured dissipation rate is often described as an approximately lognormal variable, a closer look reveals that the distribution varies due to instrumentation limitations and the local environment (Gregg et al. 1993; Moum et al. 1995; Davis 1996). In particular, the standard deviation of the PDF varies. In the thermocline, Gregg et al. (1993) found that the standard deviation of the base-10 logarithm of the measurements is smallest near the noise floor (microstructure measurements often have a noise floor around 10^{-9}–10^{-10} W kg^{-1}) and scales with the buoyancy frequency. Only correcting for these two factors, in addition to using sufficient averaging to

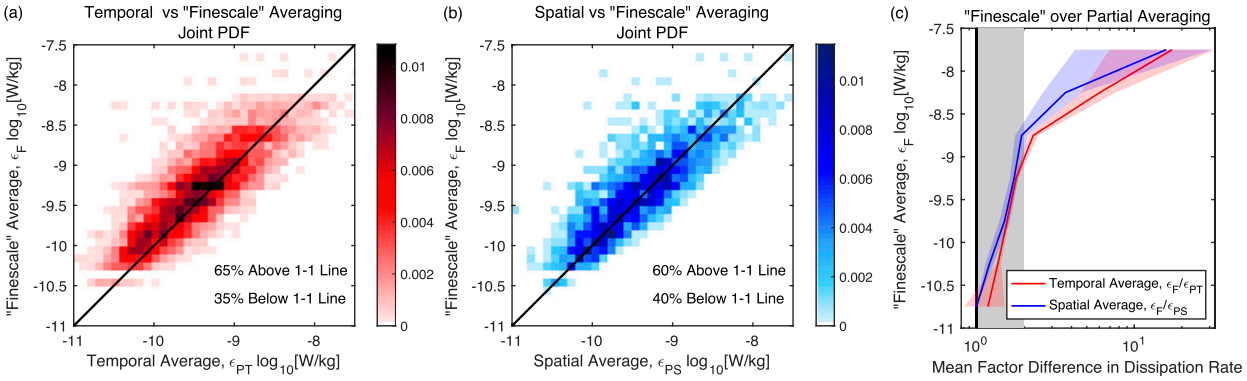

FIG. 1. Comparisons of the dissipation rates (ϵ) from microstructure that are averaged over selected time and length scales. The joint probability density function (PDF) of (a) spatial-only averaging (ϵ_{PS}, option A) or (b) temporal-only averaging (ϵ_{PT}, option B) and spatiotemporal averaging (ϵ_F, option D) on scales measured by the finestructure parameterization. The percentage of partial averages that are either higher or lower than the finescale-equivalent average (i.e., above or below the 1-to-1 line) are displayed in the lower right of each panel. (c) The ratio between the ''finescale'' averages and the temporal-only (red) and spatial-only (blue) averages as a function of the ''finescale'' averaged dissipation rate, including 90% bootstrapped confidence intervals. The black line indicates perfect agreement and values within the gray box indicate agreement within a factor of 2.

obtain uncorrelated estimates (i.e., accounting for the ''patchiness'' of ocean turbulence), will allow the microstructure observations to pass a quantile–quantile (q–q) test for lognormality in the thermocline (Gregg et al. 1993).

Over abyssal rough topography such as in the BBTRE region, the standard deviations of the dissipation rate measurements are more closely correlated with the magnitude of the turbulence (Fig. 2a) than to just the buoyancy frequency as was true in the thermocline measurements of Gregg et al. (1993). Therefore, the microstructure measurement PDF becomes wider in the presence of stronger turbulence, shifting the mean farther from the median. As the standard deviation of the distribution increases, the factor difference between the spatiotemporal ''finescale'' average and the partially averaged dissipation rate also increases (Fig. 2b). Therefore, in strong turbulence there is a larger discrepancy between the mean and the partial averages due to the larger standard deviation, which can explain the magnification in the factor difference in Fig. 1c when the turbulence is strong.

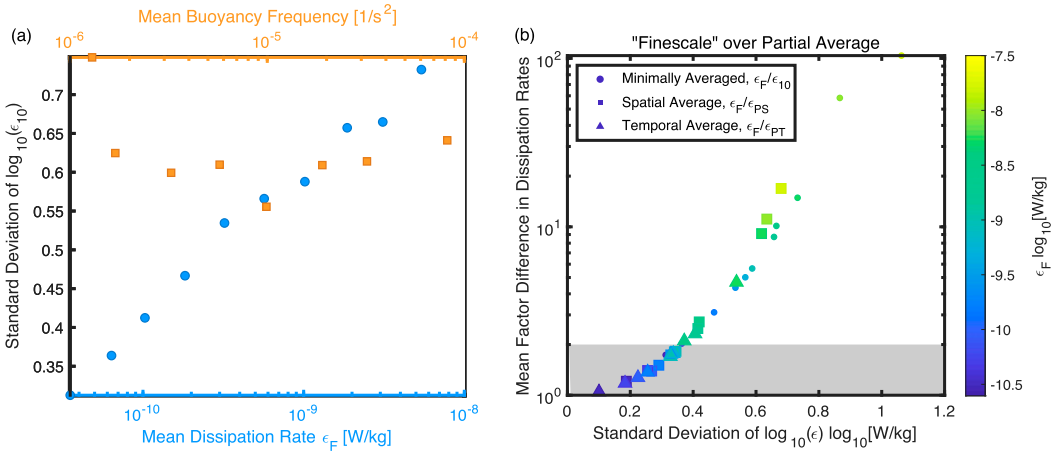

FIG. 2. (a) The standard deviation of the logarithm of the minimally averaged dissipation rate (ϵ_{10}, option C) as a function of the logarithm of the ''finescale'' mean dissipation rate (ϵ_F, option D) and the similarly spatiotemporally averaged buoyancy frequency. For the topographically diverse BBTRE, the standard deviation scales with the mean dissipation rate, as opposed to the buoyancy frequency. (b) The factor difference between dissipation rates that are ''finescale'' averaged ϵ_F and the partially averaged dissipation rates as a function of the standard deviation of the logarithm of the respective dissipation rate. The partially averaged dissipation rates include space-only averaged ϵ_{PS}, time-only averaged ϵ_{PT}, or minimally averaged ϵ_{10}. Colors are the ''finescale'' averaged dissipation rate. At least 10 values are required to plot a data point. As the distribution becomes more lognormal with increased averaged turbulence (i.e., the standard deviation increases), the factor difference between the ''finescale'' averaged and partially averaged dissipation rates increases.

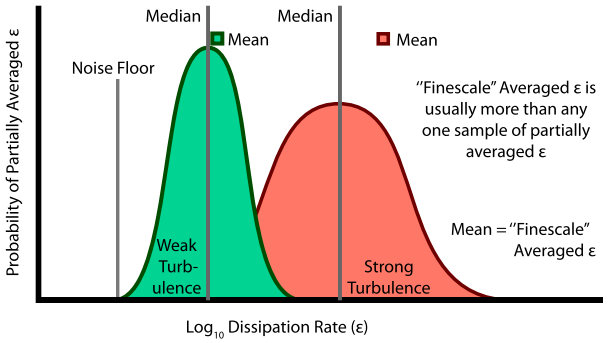

FIG. 3. A schematic example of the PDFs of the partially averaged dissipation rates (ϵ) where the environment has either weak or strong turbulence. The weak turbulence distribution is narrower because of the inherent characteristics of a weakly turbulent environment and because a larger percentage of dissipation rate measurements are at the noise floor. Since the distributions are approximately lognormal, the mean (i.e., the "finescale" averaged dissipation rate) is usually larger than any one sample in the distribution (i.e., a sample of the partiality averaged dissipation rate).

Figure 3 shows a schematic example of the PDFs of partially averaged microstructure measurements for both strong and weak turbulence. When the turbulence is strong, the mean of the partially averaged distribution is substantially larger than the median, indicating that the mean dissipation rate (i.e., the "finescale" average) will usually be larger than a single random sample (i.e., a time-only or space-only average). The systematic discrepancy between the sample and the mean produces the observed apparent bias in Fig. 1. This basic pattern also applies to the diapycnal diffusivity, since the dissipation rate is the term in the diffusivity calculation that has the smallest spatiotemporal scales.

The influence of averaging an approximately lognormal variable (with a range of standard deviations) on different spatiotemporal scales is consistent with patterns reported in many studies including Waterman et al. (2014), Ijichi and Hibiya (2015), and Takahashi and Hibiya (2019). These studies reported dissipation rates that were frequently larger using finestructure methods than for single profiles of microstructure, especially when the turbulence was strong. The results of this study suggest an alternative primary explanation for their observations: the mismatch in spatiotemporal averaging. The physical explanations originally posed by the authors may play a secondary role. In general, the influence of averaging may not always explain the entire discrepancy or explain the discrepancy in every case. For example, the observed mismatch in some studies may be in part due to choices made when implementing the finescale parameterization (e.g., Polzin et al. 2014; Pollmann 2020), or a local violation of the underlying physical assumptions of the parameterization (e.g., MacKinnon and Gregg 2003; Waterman et al. 2014). While it is important to continually test and expand our understanding of the finescale parameterization's limitations, going forward it is also imperative that this testing be done using appropriate averaging over both temporal and spatial scales following studies such as Gregg (1989), Polzin et al. (1995), and Whalen et al. (2015).

Additionally, this work highlights the importance of matching the spatiotemporal scales of the estimated dissipation rate or diffusivity with the spatiotemporal scales of the physical problem of interest. For example, using a single microstructure profile to study the meridional overturning circulation would likely underestimate the diffusivity. A finestructure profile (if the underlying assumptions are valid) would likely be a more accurate choice because the spatiotemporal scales are closer to those of the overturning circulation. Of course, averaging many microstructure profiles that are substantially separated both in space and in time would be even better. The last case would be preferred for two reasons: a larger portion of the spatiotemporal range would be sampled and the microstructure estimates that are used rely on fewer assumptions than finestructure estimates. The mixing community would benefit from carefully considering the spatiotemporal scales of the measured mixing parameters in the context of the specific physical processes under investigation.

4. Conclusions

As an approximately lognormal variable, the spatiotemporal scales chosen for averaging can have a substantial impact on the comparisons between the energy dissipation rate estimated using different methods. Since microstructure and finestructure methods produce measurements of the dissipation rate that have inherently different space and time scales, future comparisons between the two types of measurements should be averaged over similar spatiotemporal scales to ensure that equivalent quantities are being compared. Sufficient averaging has recently become more feasible due to the thousands of profiles that are publicly available in the Microstructure Database used in this study. Additionally, future work should match the spatiotemporal scales of the dissipation rate or diffusivity with those of the relevant physical processes. Studies of other variables with roughly lognormal distributions in the field of ocean mixing, such as the mixing efficiency, may also benefit from a careful consideration of the relevant spatiotemporal scales.

Acknowledgments. This work was supported by National Science Foundation Award OCE-1923558. The author thanks Stephanie Waterman, Jennifer MacKinnon, and Eric Kunze for helpful comments on an early version of the manuscript. The author also thanks two reviewers for their useful feedback.

Data availability statement. The microstructure data from the 1997 Brazil Basin Tracer Release Experiment is available on the NSF-funded Microstructure Database (https://microstructure.ucsd.edu/).

REFERENCES

Davis, R. E., 1996: Sampling turbulent dissipation. *J. Phys. Oceanogr.*, **26**, 341–358, https://doi.org/10.1175/1520-0485(1996)026<0341:STD>2.0.CO;2.

Gregg, M. C., 1989: Scaling turbulent dissipation in the thermocline. *J. Geophys. Res.*, **94**, 9686–9698, https://doi.org/10.1029/JC094iC07p09686.

——, 1999: Uncertainties and limitations in measuring ε and χ_T. *J. Atmos. Oceanic Technol.*, **16**, 1483–1490, https://doi.org/10.1175/1520-0426(1999)016<1483:UALIMA>2.0.CO;2.

——, H. E. Seim, and D. B. Percival, 1993: Statistics of shear and turbulent dissipation profiles in random internal wave fields. *J. Phys. Oceanogr.*, **23**, 1777–1799, https://doi.org/10.1175/1520-0485(1993)023<1777:SOSATD>2.0.CO;2.

Henyey, F. S., and N. Pomphrey, 1983: Eikonal description of internal wave interactions: A non-diffusive picture of "induced diffusion." *Dyn. Atmos. Oceans*, **7**, 189–219, https://doi.org/10.1016/0377-0265(83)90005-2.

——, J. Wright, and S. M. Flatte, 1986: Energy and action flow through the internal wave field: An eikonal approach. *J. Geophys. Res.*, **91**, 8487–8495, https://doi.org/10.1029/JC091iC07p08487.

Ijichi, T., and T. Hibiya, 2015: Frequency-based correction of finescale parameterization of turbulent dissipation in the deep ocean. *J. Atmos. Oceanic Technol.*, **32**, 1526–1535, https://doi.org/10.1175/JTECH-D-15-0031.1.

Kunze, E., 2017: Internal-wave-driven mixing: Global geography and budgets. *J. Phys. Oceanogr.*, **47**, 1325–1345, https://doi.org/10.1175/JPO-D-16-0141.1.

——, E. Firing, J. M. Hummon, T. K. Chereskin, and A. M. Thurnherr, 2006: Global abyssal mixing inferred from lowered ADCP shear and CTD strain profiles. *J. Phys. Oceanogr.*, **36**, 1553–1576, https://doi.org/10.1175/JPO2926.1.

Ledwell, J. R., E. T. Montgomery, K. L. Polzin, L. C. St Laurent, R. W. Schmitt, and J. M. Toole, 2000: Evidence for enhanced mixing over rough topography in the abyssal ocean. *Nature*, **403**, 179–182, https://doi.org/10.1038/35003164.

MacKinnon, J. A., and M. C. Gregg, 2003: Mixing on the late-summer New England shelf—Solibores, shear, and stratification. *J. Phys. Oceanogr.*, **33**, 1476–1492, https://doi.org/10.1175/1520-0485(2003)033<1476:MOTLNE>2.0.CO;2.

Moum, J., M. Gregg, R. Lien, and M. Carr, 1995: Comparison of turbulence kinetic energy dissipation rate estimates from two ocean microstructure profilers. *J. Atmos. Oceanic Technol.*, **12**, 346–366, https://doi.org/10.1175/1520-0426(1995)012<0346:COTKED>2.0.CO;2.

Müller, P., G. Holloway, F. Henyey, and N. Pomphrey, 1986: Nonlinear interactions among internal gravity waves. *Rev. Geophys.*, **24**, 493–536, https://doi.org/10.1029/RG024i003p00493.

Nasmyth, P., 1973: Turbulence and microstructure in the upper ocean. *Mem. Soc. Roy. Sci. Liege*, **4**, 47–56.

Oakey, N., 1982: Determination of the rate of dissipation of turbulent energy from simultaneous temperature and velocity shear microstructure measurements. *J. Phys. Oceanogr.*, **12**, 256–271, https://doi.org/10.1175/1520-0485(1982)012<0256:DOTROD>2.0.CO;2.

Osborn, T. R., 1980: Estimates of the local rate of vertical diffusion from dissipation measurements. *J. Phys. Oceanogr.*, **10**, 83–89, https://doi.org/10.1175/1520-0485(1980)010<0083:EOTLRO>2.0.CO;2.

Pollmann, F., 2020: Global characterization of the ocean's internal wave spectrum. *J. Phys. Oceanogr.*, **50**, 1871–1891, https://doi.org/10.1175/JPO-D-19-0185.1.

Polzin, K. L., J. M. Toole, and R. W. Schmitt, 1995: Finescale parameterizations of turbulent dissipation. *J. Phys. Oceanogr.*, **25**, 306–328, https://doi.org/10.1175/1520-0485(1995)025<0306:FPOTD>2.0.CO;2.

——, ——, J. R. Ledwell, and R. W. Schmitt, 1997: Spatial variability of turbulent mixing in the abyssal ocean. *Science*, **276**, 93–96, https://doi.org/10.1126/science.276.5309.93.

——, A. C. Naveira Garabato, T. N. Huussen, B. M. Sloyan, and S. N. Waterman, 2014: Finescale parameterizations of turbulent dissipation. *J. Geophys. Res. Oceans*, **119**, 1383–1419, https://doi.org/10.1002/2013JC008979.

St. Laurent, L. C., J. M. Toole, and R. W. Schmitt, 2001: Buoyancy forcing by turbulence above rough topography in the abyssal Brazil Basin. *J. Phys. Oceanogr.*, **31**, 3476–3495, https://doi.org/10.1175/1520-0485(2001)031<3476:BFBTAR>2.0.CO;2.

Takahashi, A., and T. Hibiya, 2019: Assessment of finescale parameterizations of deep ocean mixing in the presence of geostrophic current shear: Results of microstructure measurements in the Antarctic Circumpolar Current region. *J. Geophys. Res. Oceans*, **124**, 135–153, https://doi.org/10.1029/2018JC014030.

Waterman, S., K. L. Polzin, A. C. Naveira Garabato, K. L. Sheen, and A. Forryan, 2014: Suppression of internal wave breaking in the Antarctic Circumpolar Current near topography. *J. Phys. Oceanogr.*, **44**, 1466–1492, https://doi.org/10.1175/JPO-D-12-0154.1.

Whalen, C. B., L. D. Talley, and J. A. MacKinnon, 2012: Spatial and temporal variability of global ocean mixing inferred from Argo profiles. *Geophys. Res. Lett.*, **39**, L18612, https://doi.org/10.1029/2012GL053196.

——, J. A. MacKinnon, L. D. Talley, and A. F. Waterhouse, 2015: Estimating the mean diapycnal mixing using a finescale strain parameterization. *J. Phys. Oceanogr.*, **45**, 1174–1188, https://doi.org/10.1175/JPO-D-14-0167.1.

Wijesekera, H., L. Padman, T. Dillon, M. Levine, C. Paulson, and R. Pinkel, 1993: The application of internal-wave dissipation models to a region of strong mixing. *J. Phys. Oceanogr.*, **23**, 269–286, https://doi.org/10.1175/1520-0485(1993)023<0269:TAOIWD>2.0.CO;2.

Winkel, D. P., M. C. Gregg, and T. B. Sanford, 2002: Patterns of shear and turbulence across the Florida Current. *J. Phys. Oceanogr.*, **32**, 3269–3285, https://doi.org/10.1175/1520-0485(2002)032<3269:POSATA>2.0.CO;2.